A Multi-Classification Deep Neural Network for Brain Tumor Images

Mrs. MUTYALAPALLI KANAKA DURGA[1], Mr. L.V.S. NARAYANA[2], Mrs. K. SATISHA[3] ASST PROFESSOR[123]
DEPARTMENT OF ECE,
SWARNANDHRA COLLEGE OF ENGINEERING AND TECHNOLOGY, NARASAPUR

ABSTRACT

In order to evaluate the lesions and determine the most effective treatment, brain tumor classification is crucial. There are several imaging modalities that may be used to detect brain lesions. On the other hand, MRI's high-quality pictures and lack of radiation make it a popular choice. The subfield of machine learning known as deep learning (DL) has recently shown remarkable efficacy, especially in classification and segmentation. Here, we propose a convolutional neural network–based deep learning (DL) model for brain tumor classification using two publicly available datasets. Malignant tumors are categorized by the former, which includes meningiomas, gliomas, and pituitary tumors. Second, there's the system that divides gliomas into three different grades: II, III, and IV. There are two datasets available; one contains 3064 T1-weighted contrast-enhanced photographs taken by 233 patients, and the other 516 images taken by 73 individuals. In both tests, the proposed network architecture achieved better results than the state-of-the-art approaches, with 96.13% and 98.7% accuracy, respectively. The results demonstrate that different kinds of brain tumors may be classified using the algorithm.

INTRODUCTION

An abnormal and uncontrolled brain development is the very definition of an anomaly.expansion of brain cell volume. It is physically difficult to influence human performance via organ/tissue specificity due to the inflexibility of the human cranium and other physical constraints.and it has the potential to metastasize, or spread, from the brain to other organs.in an effort to influence people's actions [1]. The most recent data from the World Health Organization (WHO) indicates that just 2%of people are found to have a brain tumor, according to the World Cancer Survey.when the stakes are very high in terms of potential harm or death [2].Cancer Research UK Supporting Organisation, Male Approximately 5,250 people die each year in the UK as a result of cancers affecting the brain, spinal fluid, or brain stem [3].As an example, brain lesions may be classified using a variety of approaches.malignancies that are not of the main or secondary kind. About 70% of brain tumors are classified as tertiary. This accounts for about one-third of all cases.With a 30% surplus rate. Tumors, like most malignancies, originate in the nervous system, and this classification is meant for use with them.the main arteries of the body harboringtumors. Malignant secondary development, however, unfortunately predominates in the statistics, and malignancies begin in impulses sent to the brain fromother regions of the body [4].The work will be examined by the assistant editor, and Yutong Zhang authorized its final publication.Our need for a system to categorize brain tumors necessitates the employment of many testing methodologies. One of the most common diagnostic tools, however, is magnetic resonance imaging (MRI).standard procedures that avoid harming the substance being processed. The origins of the magnetic resonance imaging (MRI) trendThere was no usage of any radioactive material that may be harmful in the scanning process.in addition to its remarkable transparency in soft tissues and its capacity to accommodate several exposures or the addition of compounds that enhance contrast, as described in [5] and [6].The vast majority of brain cancers, known as gliomas, begin in the brain's glial cells [7]. Illustrations of Different GliomasSome estimatesput the percentage of tumors that originate in the central nervous system (CNS) at 30%.Cancers of the meninges [7]. A total of four categories characterize gliomas.according to the World Health Organization's divisions (I through IV) [8]. Level ofMalignant type I masses resemble benign tumors in both look and texture.Glial cells of grade II are chemically extremely similar to those of grade I.Atypical characteristics are seen by grade III malignant tumors.glioblastomas are the most

aggressive of the grades I–IV tumors, and there are also visible cellular shape abnormalities [1].A meningioma is a malignant tumor that develops on the brain's protective barrier.encompasses the space inside the skull that develops in a peaceful manner and houses the central nervous system. The majority of meningioma-related tumors are considered benign [8].Cancers of the pituitary gland, in contrast, develop within the glands themselves. Substances that control physiological functioning. Actually, it's doable.very severe, very dangerous with bone tumors, and moderateA pituitary tumor has the potential to influence hormone production over an extended period of time.

disability or loss of vision [1].

Early identification is crucial in light of the existing data.

Critical tasks now include the diagnosis and categorization of brain tumors.

assessment of the problem and recommendations for enhancing a straightforward remedy that has contributed to the preservation of many lives [8]. Additionally, sorting items into categories may be a tedious and time-consuming process.Doctors and experts have a bigger challenge when dealing with complex medical cases. Expert help is required for diagnosis, location, and treatment in such instances.First, the tumor cells are compared to their environment and then filtered.In Order To Make Them More Comprehensible To TheAudiencesense and reach a final decision; in the case of a development, for example, whether we can classify it. Despite the monotony of the job, CADsoftware will save you a ton of time and energy.Braintumors may be detected early with the use of a computerized system.reducing the rate at which people need to step in.Learning statistical processes for accomplishing a certain objective without explicit instructions and instead relying on tried and verified patterns is the study of computational models, which includes programs and data structures (ML) [9]. The medical imaging business has recently used machine learning techniques as a subsystem of artificial intelligence [6]. Separated into managed and wild groupings are the two main ways to classify it. A translation function may be calculated in a number of ways with the right kind of instruction and the right kinds of technological techniques.factors, together with the names of the results we anticipate from themI changed the names of the subjects. Similar to a support vector machine (SVM), a neural network (NN) [10], or K-nearest neighbours (KNN) [11], independent study is the main computer-aided pattern recognition in the course materials.Using SOM, the System ObjectModel, and the concepts of self-organization and imprecise c-means [12], we take directed learning's output into account, but not its input. Greyscale, flat, and motionless are the hallmarks of most instructional graphics.statistics that improve learning and have the potential toTumor division often occurs before feature extraction. These components are considered "handcrafted" due to the meticulous attention to detail that went into their making. A specialist in the field may determine which components are most important by devoting years of research and expertise to the topic. On topof that, managing tasks like these may be tedious and prone to mistakes. Gathering data on a vast scale [14].Learning data description and feature hierarchies is fundamental to Deep Learning (DL), a subset of Machine Learning (ML).Deep learning techniques rely on characteristics for feature retrieval utilizing nonlinear processing, which is a hierarchical structure. The output of the A layer is fed into the input of the layer below it. We can draw better generalizations as we discover more details.association [15]. Convolutional neural networks, or CNNs, are one kind of artificial neural network.popular DL application in the domain of picture analysis, and it was constructed in a manner that needed very little preparatory work [16]. Data presented in a variety of matrix shapes influencesit, as do studies of the human brain [17]. cited as [18]. A deep convolutional neural network was used for the first time to solveThere has been a noticeable upturn in the popularity of theIt was Lacuna whofirst proposed the concept of a deep neural network towards the end of the twentieth century.Text recognition software use lent as a tool.upon 1998 [19]. A deep convolutional neural network employing (ImageNet LSVRC-2010) a set for picture classifications eventually helped it gain momentum after a long wait.Alex Net [20] is being used as a methodology. What makes Alex Net so exceptional is that

contrasts with other prevalent network designs

stage of existence. A spinoff series was born because of its popularity. Case studies of successful deep learning implementations with CNNs.Unlike conventional computers, CNNs are capable of producing very accurate results, and their capacity to learn new characteristics is one of their primary strengths.We are close to achieving both learning and basic neural networks.When there is a greater amount of data available for analysis, efficiency rises.[6] The model is precise and dependable. One drawback of the traditional CNN layout is that itFeature extractors and convolutional filters are bothin use at the moment.We are removing more complicated elements as we go deeper.(Details on physical locations and ideas). Styluse Disentanglement via Merging the Outcomes of Multiple Small FiltersLater, we will start by determining which characteristics are most important, and then we will begin training the identification network. cited as [18].Many different techniques have been proposed for classifying brain tumors. Machine Learning using Image Data and AlgorithmsTime passes. A method was suggested by Zacharaki et al. [21] in 2009.Separation of grades using support vector machines and kernel neural networks may help move glioma classification beyond a yes/no paradigm.The overall accuracy of the classification is 88%, with a multi-classified accuracy of 85%.about a binary choice. Early on, El-Dashan et al. [22] presentedExamination of eighty brain tumors, with each tumor type classified as either benign or abnormalAs an example, DWT is a method for mining digital picture data.characteristics, data distillation using Patriates, artificial neural networks (ANN), and lastly kernel neural networks (KNN) for picture labeling; 100% reliability for 98% and 99%. Chang et al. [23] suggested a way to improve cognitive ability in 2015.increase the accuracy of tumor grading by strengthening the tumor area by first zooming out and then dividing the picture into more manageable parts. In order to identify unique traits, the specialists employed three methods:combined accuracy rating of 91.28% combining ring-shaped tumor segmentation and density matrix of grayscale occurrences and co-occurrence matrix (GLCM) for optimum precision when used in conjunction with the BOW

lengthening a specified region.

A remedy is suggested by Ertegun and Rubin [24] in their paper.Different types of gliomas were classified by the authors using CNN.medical pictures (II, III, and IV), and another assignment labelinggliomas as HG or LGG (LGG).Handling Glioma Grades (HGG). The level of accuracy reached 71% or higher.The degree of association between the two is 96%. An example of a sagittal brain tumor was used as a model by Paul et al. [25].examples for learning and practicing the two primary types of classificationonto data classification using a convolutional neural network (or "convnet"), which is the product of combining two layers, two max-pooling layers, and several convolutional layers—the first two of which are fully interconnected—with a third stratum that getsas close as 91.43% to the actual value, at most. To wrap things up, Afshar et al. [26] demonstrated a container network called Caps Net that combines categorization using brain and protrusion tissue MRI.Brain development became more stable. The success percentage for our services is 90.89 percent.During the course of this investigation. In their investigation, Anarkali et al. [27] suggested similar approaches.A classification method for brain tumors is developed using only two principles.neural network and a genetic algorithm's visual representation (GA-CNN),We achieved an accuracy rate of 90.9% on the first test scenario.

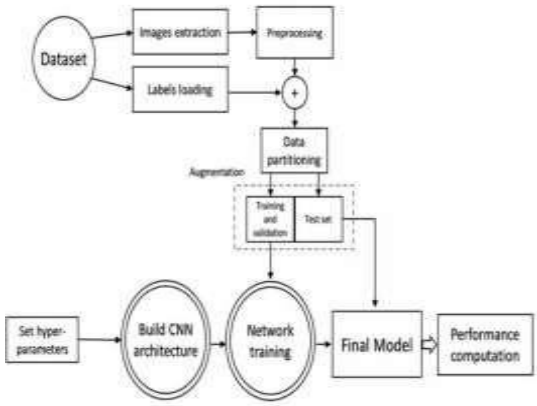

FIGURE 1. Block diagram of the proposed method.

Although these parameters were satisfied in the second case study, a 94.2% accuracy rate was reached when classifying gliomas as either glioblastoma, meningioma, or pituitary tumors. The authors of this piece propose a CNN architecture for use in classification tasks. Various kinds and stages of malignant brain tumors. The network's architecture is fine-tuned by experimenting with severalconfigurations until you find the one that works best for you. For this presentation, we have included an outline.Following this, Section 2 provides a detailed description of the proposed method, including everything from the preliminary data gathering to the modifications made to the CNN algorithm to make it compatible with the tools and resources used for this research. The results and discussion are covered in Chapters 3 and 4, respectively, before Part 5 concludes the work.

METHOD

You may see the building components of the proposed process in FIGURE 1.in which the system begins by loading images and extracting names from dataset raw files, and then immediately after datasets are sorted into groups for instruction, testing, and evaluation, it performs cleaning and enhancement procedures. Afterwards, the structure ofIt is provided once the need of the proposed method has been established.enhancement, regularization techniques, and hyper-ink algorithm. Training and network efficiency will be our last topics.You may see the outcomes of the calculations.

DATASET

We use two datasets in our investigation. The following is the first data collected from Nanyang Hospital and the General Hospital:The Tianjin Medical Institute in China from 2005 to 2010 [23].many versions of it were subsequently made available online.2015, with the 2017 release of the last installment. Information originimages that have had their contrast and T1 weights adjustedtumors of the pituitary gland, meningioma, and glioblastoma, with 233 cases reported [28]. There are a number of variables that may affect the size, location, and appearance of brain tumors.shown inFigure 2 (a) according to their respective categories.The collection includes oblique, axial, and sagittal viewpoints.You may see the axial and transverse views (b) in Figure 2. The secondaryOne publicly available source of information is the Cancer Imaging Collection (TCIA) [29]. Remberandt, the Central Database of Molecular Data on Big Brain Tumors.videos including 130 people with diverse backgrounds in terms of age, gender, race/ethnicity, and education level [30]. Grades II, III, and IV glioblastoma T1-weighted enhanced contrast pictures were used for image selection.Image 3. In Tables 1 and 2, you can find more details about the two databases and their respective descriptions.

STAGE PRIOR TO PROCESSING

To ensure that the suggested framework is capable of handling the input pictures, a pre-operation is carried out. The initial step is a down-compress the original 5125121 picture into1281281 pixels to reduce dimensions, compressing com-potations and aid the network in functioning more

effectively.requiring less effort and time and leading to simpler computations. Then,In order to keep the system running smoothly, data is jumbled before being divided.training on uncategorized data to avoid overspecializinga particular data set's band size. The information is presented in three parts;Each of the three sets—training, certification, and testing—has its own uniquecategories to aim for (68% in instruction, 32% in testing, andvalidation). At last, we enhance the pictures used in scientific researchthat they are distinguishable as fresh by the system, andcommonly employed to prevent model overfitting and boost robustnessness [20], [31]. Furthermore, this linear improvementThe pictures are distorted by adding a monochrome noise effect (sodium noise).

PICTURE 4 compares the enhanced examples given here with the

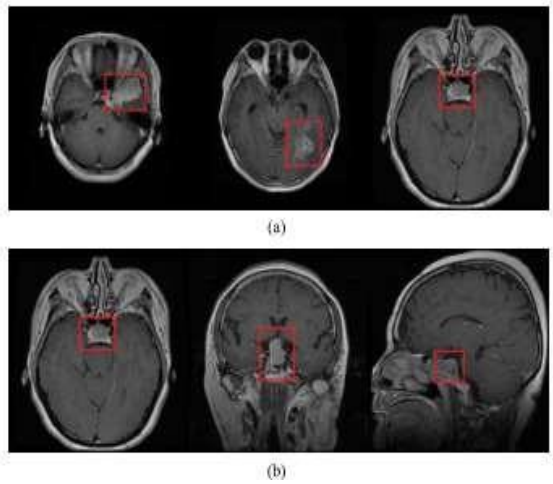

FIGURE 2. (a) Different three axial brain tumour types as follows; in this series of images, wefirst see (a) a meningioma, then (b) a glioma, and finally (d) three different obtained views of the pituitary tumour, in the axial, coronal, and sagittal planes. The Sarcomas are.

within the confines of the crimson square's boundaries.

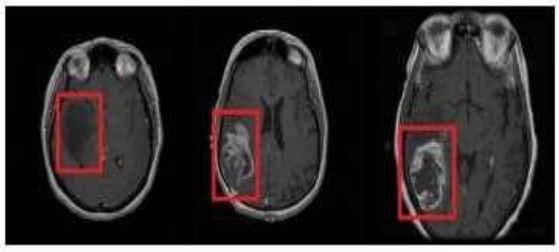

FIGURE 3. Different glioma grades included in REMBRANDT dataset (Grade II, Grade III and Grade IV from left to right respectively). Tumours are localized inside.

ared rectangle.

TABLE 1.***Number of slices for each brain tumour type (meningioma, glioma and pituitary) in dataset I and their corresponding number of patients.***

Tumor Category	Number of Patients	Number of Slices
Meningioma	82	708
Glioma	91	1426
Pituitary	60	930
	233	**3064**

original one; for study I, we flipped it on its x-axis, mirrored it right to left, added salt noise, and rotated the picture by 45 degrees. Using this method of enhancement, our finished collection included 15,320 pictures for Study I and 516 images for Study II, an increase of a factor of 5 from the initial 3064 images.

PROPOSED CNN ARCHITECTURE

The suggested CNN architecture is depicted in FIGURE 5. The first of its 16 levels store the enhanced pictures from the previous pre-processing phase, the input layer.using activation functions of convolution layers

TABLE 2. Number of slices for glioma grades in dataset II and their corresponding number of patients.

Tumor Category	Number of Patients	Number of Slices
Grade II	33	205
Grade III	19	129
Grade IV	21	182
	73	516

the layers used for convolving, Rectified Linear Unit (REL) normalizing, pooling, and selecting features. A dropout layer is used to avoid overfitting.and then a completely linked layer, a SoftMax layer for output prediction, and finally a classification layer for generating the expected class. Here's how we break down each layer: To begin, we use the input layer to verify the input pictures' sizes and implement a data standardization [20]. The suggested design features three convolutional layers. Sliding K convolutional filters (kernels) of size (M N) are applied to the input pictures in a 2D convolutional layer, and the dot product of the weights (kernels) is calculated.

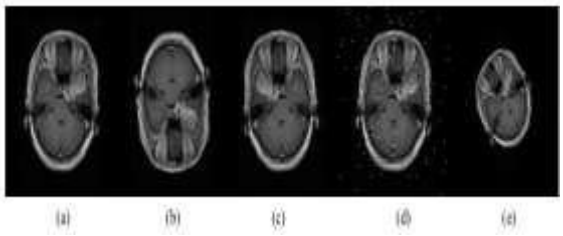

FIGURE 4. (a) The original image, (b) up-down flipping, (c) right/left mirroring, (d) add salt noise to the image, (e) rotating by 45 degree.

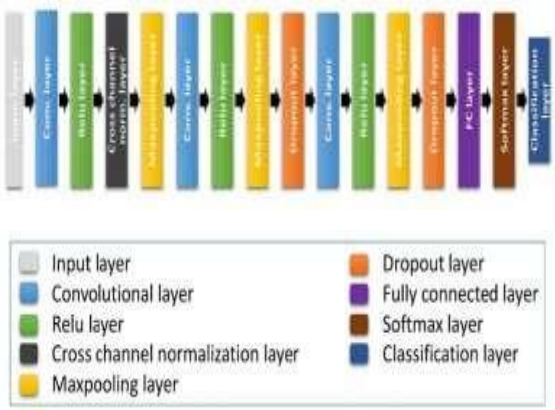

FIGURE 5. The proposed CNN architecture.

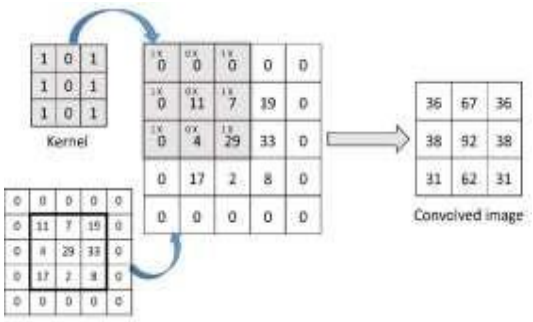

FIGURE 6. Convolutional layer example (input: 3×3, zero padding: 1, kernel size: 3×3, Stride: 1, output: 3×3).

components (input, weights, and input). The horizontal and vertical steps that the filters take as they traverse the image are referred to as stride (S). Before dragging the filters over the basic photographs, they might be padding them with zeros (P).that information may remain on the perimeter. Feature identifiers like these kernels work by detecting lower-level features (such edges, lines, and clumps) in the first layers and higher-level features in the subsequent layers [19].Input measurements of 3 3 are produced by superimposing a 3 3 kernel (in dark) over a 3 3 image, as shown in Figure 6. For the convolutional layer, set P = [0,0,0,0], [2,2,2,2], and [2,2,2,2]; for the pooling layer, set P = [0,0,0,0], [2,2,2,2], and [2,2,2,2]. For K = 64, 128 and M N = 10 but 3 3 and 2 2 are the values. S = [1, 1].

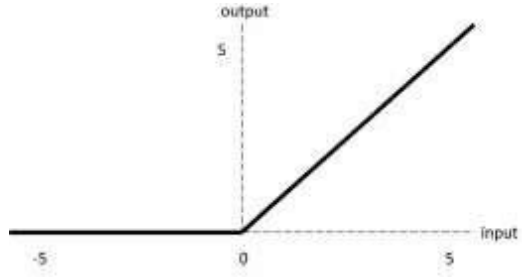

FIGURE 7. REL activation function.

First, second, and third are the levels in sequence. Every convolutional layer is followed by a non-saturated activation function termed REL to significantly reduce training time. In the presence of additional activation functions [20, 32, 33]. Here is an equation for the REL model as a function of x: when x is positive, the output is the same as the input, and when x is negative, the output is zero [33]. f (x) = max (0, x) 69219 is the REL function, as seen graphically in Figure 7.After that, a cross- channel normalization layer scales and modifies the active-tons to normalize the input layer. By using a channel-wise frame of a predetermined size (in this case, 5), it adds an adjustment layer to the local response. Standardization aids in speeding up backpropagation and training networks [20, 32].

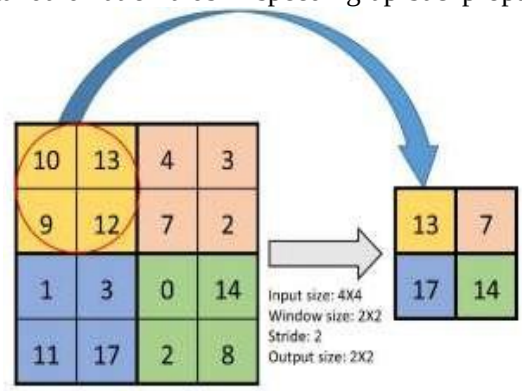

FIGURE 8. Example of a max-pooling layer (the maximum value out of a

perspective (only matching hues are considered).However, the Maximum Pooling layer is a down-Spatial invariant sampling method that achieves this by randomly dividing the image into squares (2 by 2 in the proposed form), scooting over it with an intentional step (2 2), and finally concentrating onthe best feasible outcome. These are the four main components. In the linkage, a pooling layer is used to reduce factors and, therefore, computations [34, 35]. Pictured in Figure 8 is the max-pooling layer.Figure 9 is an example of how to exit layering to reduce the chance of overfitting.Eliminating superfluous activations (nodes) is the job of this layer.to the Ing step at random, which also helps the train's speed a lot [36]. The best loss rates in the proposed design were 10% and 20%, as we found out.amounts of dropouts in layers 1 and 2.Next, we implemented three state-of-the-art components: the FC, the SoftMax layer, and the Completely Con-classification layer. By connecting all of the neurons in one layer to each cell in another, the former produces the latter's output.This stratum is composed of three kinds. On completion of the (normalized exponential) SoftMaxlayer.function, the FC stratum is reached. With a total of 1 (100%) to another value, all of the predicted data is compressed using a SoftMax layer with integers ranging from 0 to 1. This layer's may be calculated.

result.in this way:

It is possible to determine the likelihood of any group (j) by using (k)the aggregate of squares for all classes plotted against y (z).proportions are 1, as depicted in FIGURE 10. Finally,we use a cross-entropy based classification layer.loss to calculate an approximation of the classificationexpected class title for each of the supplied pictures. Damage cantarget identifiers p can be determined using equation (3).vector, and q (x) represents the SoftMax layer's final output vector.

$$H(p,q) = -\sum_{x} (p(x) * log(q(x))) \quad (3)$$

REGULARIZATION TECHNIQUES ANDOPTIMIZATION ALGORITHM

Regularization ensures a good fit of a solution function during training by preventing system overfitting. Several techniques have been developed to prevent overfitting during the preproduction stages, including the pausing and training phases. Data enhancement, which involves introducing a geometric and color distortion to the original photographs, may be used to avoid overfitting [23], [31],[38]. The next step was to test out several network architectures to see which one would result in the simplest network. Then, using dropout layers, the hidden unit weights may be randomly deleted [36], [39]. One way to punish the cost function and add weights decrease using L2 regularization is as shown in the following equation [40].

$$Cost\ function' = Cost\ function\ (Loss) + \lambda \sum_{i=1}^{k} w_i^2 \quad (4)$$

where is the regularization parameter (specified hyper-parameter), and w is the weight(s) associated with iteration I from 1 to last but not least, the "early halt method" has been implemented in a few tri-training is terminated prior to the end of a period if the system is stable or if overfitting is detected by an auxiliary learning system (also) [40].

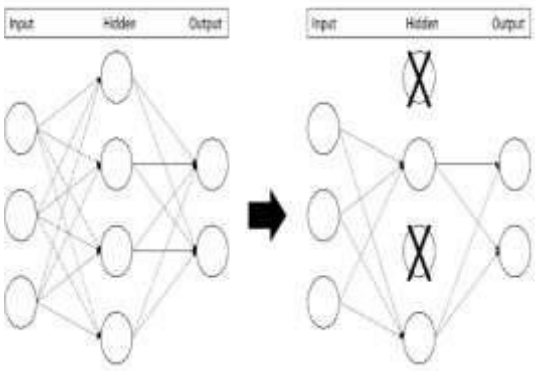

FIGURE 9. Example of dropout layer (probability of 50% appears on the right).

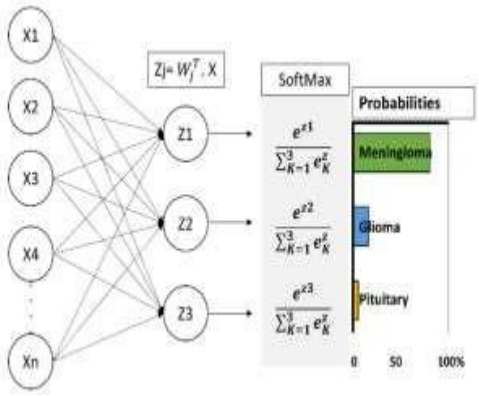

FIGURE 10. Example of Soft-max layer.

Optimizing a network typically entails making minor, incremental changes to the negative gradient until the loss function is at its world minimum.net (convergent) path [41]. For the suggested architecture, we discovered that the "stochastic gradient descent with momentum" is the best algorithm.

EXPERIMENTS AND RESULTS

In PICTURE 11, we can see the improvements and decreases in accuracy that our proposed network went through during the assessment phase of research I. Shown in EXHIBIT 11(a) is the achievement of virtually perfect accuracy after only 5,000 attempts. During the testing period, the accuracy reached a top of 96.13% and a maximum of 8550 iterations, approaching 100%. As seen in Figure 11(b) of the loss graph for mini-batches, the slope lowers suddenly at the beginning before exhibiting minor variations, which is expected given the small size of the mini-batch. In most cases, these fluctuations disappear after 6400 cycles, and the loss curve approaches zero.

During the confirmation stage, EXHIBIT 12 shows the increases and losses in accuracy that study II experienced. After only 100 trials, complete accuracy was achieved, as seen in FIGURE 12(a). Consequently, 98.7 percent was the maximum degree of accuracy reached throughout the testing phase. The loss histogram for mini-batches shows a sharp drop, as seen in Figure 12(b).

This dip usually goes away beyond the hundred mark.

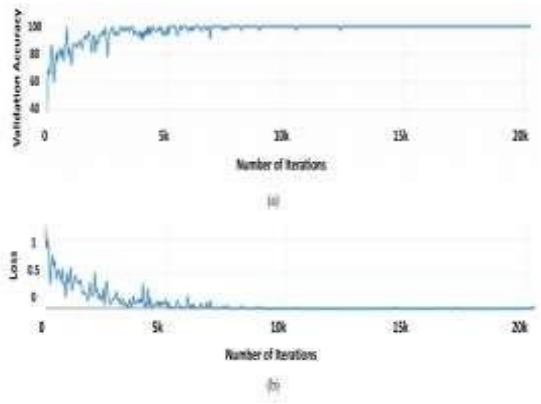

FIGURE 11. Validation accuracy and loss over the whole training iterations of study I: (a) Validation accuracy (higher is better), and (b) Loss (lower is better).

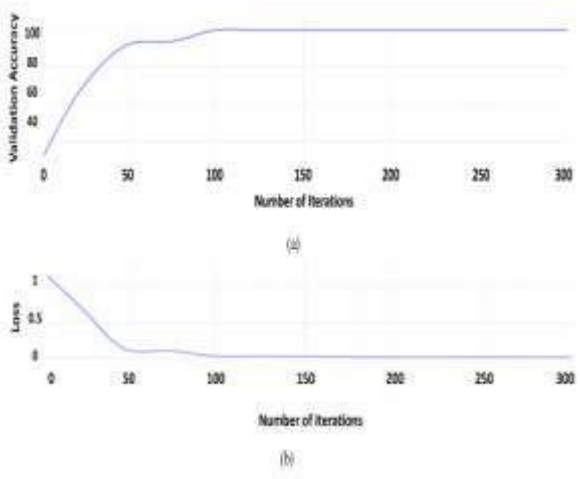

FIGURE 12. Validation accuracy and loss over the whole training iterations of study II: (a) Validation accuracy (higher is better), and (b) Loss (lower is better).

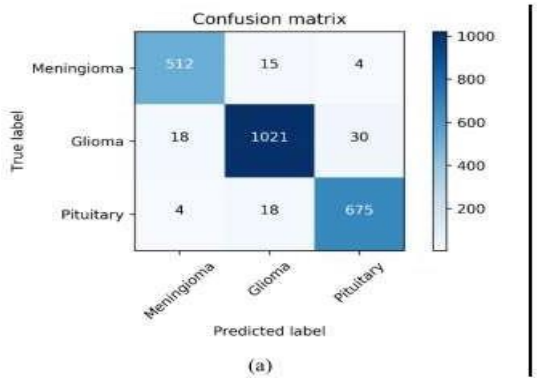

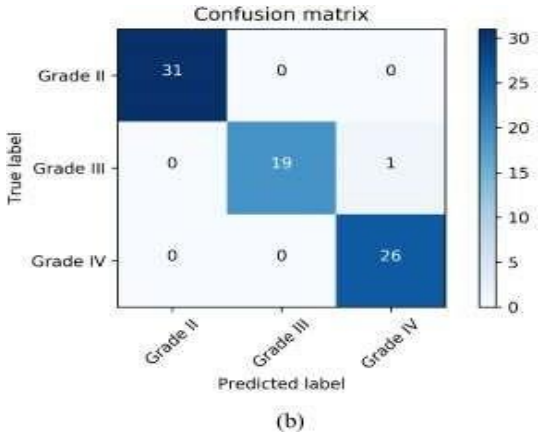

(b)

FIGURE 13. The confusion matrix of theproposed model: (a) for study I, and (b) for study II.*TABLE 3. Accuracy metrics in terms of TP, TN, FP, FN, precision, sensitivity, specificity, and accuracy.*

Method \ Metrics	Tumor Type	TP	TN	FP	FN	Precision	Sensitivity	Specificity	Accuracy	Total no.
Proposed Model for Study I	Meningioma	512	1744	22	24	0.958	**0.955**	**0.987**	**97.54%**	547
	Glioma	1021	1195	33	61	**0.972**	0.944	0.951	95.81%	1069
	Pituitary	675	1566	34	48	0.952	0.934	0.97	96.89%	697
Proposed Model for Study II	Grade II	31	46	0	0	1	1	1	**100%**	31
	Grade III	19	57	0	1	1	0.95	1	99%	20
	Grade IV	26	50	1	0	0.963	1	0.98	**100%**	26

CONFUSION MATRIX

Confusion vectors summarizing system performance across both trials are depicted in FIGURE 13. (I and II). Predicted values (system output) are shown along the X-axis, while actual values The real markings can be seen along the Y-axis (ground truth). Equation 5 was used to determine the values for precision, sensitivity, specificity, and accuracy.

$$Precision = \frac{TP}{(TP + FP)}$$
$$Sensitivity = \frac{TP}{(TP + FN)}$$
$$Specificity = \frac{TN}{(TN + FN)}$$
$$Accuracy = \frac{TP + TN}{(P + N)}$$

were,

True Positive (TP) refers to the number of instances when the results are positive, which is the percentage of positive situations that were correctly anticipated. When someone uses the term "real negative," what does it imply then? Situations, and they're not exactly hopeful when you give them some thought.Getting a positive outcome while you were expecting a negative one is an example of a type two mistake. When a result is expected to be positive but is really negative, it is termed a type one mistake or a false positive (FP).Table 3 displays the precision metrics that were collected from the uncertainty matrix. The top performers in terms of accuracy, sensitivity, specificity, and precision are

shown in Table 3. Melanoma, glioma, and meningioma all have very high success rates: 96.69%, 95.74%, and 95.71%, respectively.

ABLE 4. Different architectures and hyper-parameters tested and tried before reaching the final model.

Factor(s)	Values
Number of convolutional + ReLU layers	1, 2, 3, 4
Number of cross-channel normalization layers	1, 2, 3
Number of drop out layers	1, 2, 3
Maximum epochs	20,40,50,60,80,100
Number of fully connected layers	1, 2, 3
Number of convolutional kernels	8, 16, 32, 64, 128, 256
Kernel size	2, 3, 5, 7, 9, 10, 11
pooling layer	Max pooling, average pooling
pooling layer window size	2, 3, 4, 5
Optimizers	SGD, Adam, RMSprop
Mini-batch size	1, 4, 8, 16, 32, 64, 128
Dropout rate	0.1, 0.15, 0.2, 0.25, 0.5
Initial learning rate	0.01, 0.001, 0.0001
Learning rate drop factor	0.1, 0.2, 0.3

TABLE 5. Comparison between the proposed model and previous related works.

	Model	Best Accuracy for Study I	Best Accuracy for Study II	Classification Type	Classification Method
1	Cheng et al.[23]	91.28%	-	Multi	SVM and KNN
2	Paul et al.[25]	91.43%	-	Multi	CNN
3	Afshar et al.[26]	90.89%	-	Multi	CNN
4	Anaraki et al.[27]	94.2%	90.9%	Multi	GA-CNN
5	Zacharaki et al.[21]	-	85%	Multi	SVM and KNN
6	Zacharaki et al.[21]	-	88%	Binary	SVM and KNN
7	El-Dahshan et al.[22]	-	98%	Binary	ANN and KNN
8	Ertosun et al.[24]	-	71%	Multi	CNN
9	Ertosun et al.[24]	-	96%	Binary	CNN
10	Proposed structure	**96.13%**	**98.7%**	Multi	CNN

Pituitary classification. However, we achieved an accuracy of 100% in classifying glioma Grade II, 95% for glioma Grade III and 100% for glioma Grade IV.

EMPIRICAL ARCHITECTURES AND HYPER-PARAMETERS

In this section, we detail the many design considerations that go into creating these building choices. Table 4 displays the outcomes of these early experiments.finishing the best-possible framework presentation in terms of performance.

TOOLS AND TIME CONSUMPTION

The proposed deep neural network architecture is trained on an NVIDIA GTX 1060 Processor (with 6 GB of memory) using MATLAB 2018b, Python, and 16 GB of RAM. What follows is the instructionalTwo studies, one with 2,89 minutes of data and 10,417 photographs, and the other with only 2.5 minutes of data and 350 images, were conducted. The average runtime of the tests for Research I was 8.5 ms and for Research II it was 9.6 ms per image.

DISCUSSION

The many types of brain tumors are described in detail.Tumor categorization is proposed using a model of a convolutional neural network.by the use of X-ray images for comparison. The CNN modelis affected by a lot of things.so that the system may be configured before the design is finished.texture. Starting from scratch when training a network is notoriously tough.produced in a

matter of minutes, days, or weeks.While avoiding tampering with the data in any way. Results from Previous Research with Similar Brain Tourniquet Setups, Hyper-Settings, and Levels: Table 5. A number of benefits of the proposed design are readily apparent. Among other methodologies, it produces the most accurate predictions. The advantages of inferred structure have been shown in earlier studies. The proposed CNN method is suggested for use in classification. Using a straightforward approach, we can show how the brain grows into something well-connected to it.But in order to extract the features mentioned in [21–23] and apply them in, feature engineering was used. Here we go to the next tier of categorization. Despite the authors' obvious usage of GA to represent network structure, the accuracy of GA's predictions was not higher than that of traditional approaches ([27]). The authors in [25] only make use of two convolutional layers.CPUs with 64 separate cores. Furthermore, they are staffedFour distinct tiers of significant loss have been identified. Connected devices. Training networks with messed up visuals has so far proven ineffective, according to Ertegunand Rubin [24], even if this has been done using pathos-logical reasoning.discovered by merging the output of two separate applications. The authors have also used tumors with fuzzy edges in [26].information that may help the system show results more precisely. In the preceding identification phase, human interaction is necessary.working as a reporter without proper training is risky. We've Made It Through, To An Extent, However,

The suggested technique achieves encouraging classification findings.

These findings need to be verified with larger databases. Recruit from both gender and all walks of life to widen its appeal. And eventually try it out for other medicinal applications. Not only that, but the framework of the method is not transferable between lessons. Simplifying a limited set of pictures is a common task in deep learning. Ing restrictions, but rather the method can be adjusted to meet the needs of the individual fine-tuned after extensive data training to affect subtle details dataset.

CONCLUSION

This work introduces a CAD approach for classifying magnetic resonance images of brain tumors as either meningioma, glioma, or pituitary.Gliomas are categorized into classes II, III, and IV using a particular architecture of deep neural networks. A total of sixteen layers make up the proposed network; the first layer contains the pre-processed images; the remaining levels include three convolution layers, three REL layers, a normalization layer, and three Carpooling layers. Furthermore, the output is forecasted by a fully connected layer and a SoftMax layer; the predicted class is generated by a class-fiction layer; and two dropout layers are used to prevent overfitting. Due of the variety of imaging views, the relatively modest dataset was able to exhibit enhanced conclusions via data improvement. Our proposed design achieved a 96.13% and 98.7% level of accuracy with the two datasets used in this investigation.

REFERENCES

[1] *For example, "brain tumors" by L. M. De Angelis January 2001, volume 344, issue 2, pages 114–123, New England Journal of Medicine.*

In their 2014 World Cancer Report, B. W. Stewart and C. P. Wild cite [2]. The International Atomic Energy Agency (IARC), 2014. Lyon, France.

[3] Statistics on Brain, Other Central Nervous System, and Intracranial Cancers. May 2019 access.[On the web]. This resource is accessible at: https://www.cancerresearchuk.org/.[4] J.-Y. Delattre, "Pry-Mary brain tumors in adults," A. F. Carpentier, K. Hoang-Xuan, and A. Behin The Lancet, 2003, vol. 361, no. 9354, pp. third-third.

[5] A. Defleas, H. Correlation-Based Imaging of Brain Tumors. Press of Springer, Berlin, Germany, 2002.

The authors of the cited work are Listens, G., Kooi, B., Bernarda, A., Ciampa, M., Ghafoor, Ian, and Setia, J. A. "A survey on deep learning in medical image analysis," published in December 2017 in Med. Image Anaal., by W. M. van der Laak, B. van Ginneken, and C. I. Sánchez, 42(60–88) pages.

Cancer Genet., vol. 205, no.12, pp. 613-621, Dec. 201269224, by M. L. Goodenberger and R. B. Jenkins.May

[8] "The 2016 World Health Organization classification of tumors of the central nervous system: A summary," Acta Neuropathology, vol. 131, no. 6, pp. 803-820, Jun. 2016, C. Ohtaki, O. D. Wrestler, P. Kaliese, G. Reifenberger, A. von Deimling, D. Figarella-Branger, W. K. Cavenee, H. Ohtaki, and D. W. Ellison.

"Pattern Recognition and Machine Learning" by C. Bishop [9].Springer-Verlag, 2006, Berlin, Germany.

In the proceedings of the 2013 International Conference on Advanced Nanomaterials and Emerging Engineering Technologies (ICANMEET), T. Rajesh and R. S. M. Malar presented a paper titled "Rough set theory and feed forward neural network based brain tumour detection in magneticresonance images," which runs from pages 240 to 244.

The paper "MRI brain cancer classification using hybrid classifier (SVM-KNN)" was presented at the 2015 International Conference on Industrial Information Control (ICIC) and can be found on pages 60–65. The authors are K. Machala, H. B. Anandpur, V. Kapur, and L. Kosta.

12 "MRI brain image segment-station using modified fuzzy C-means clustering algorithm" by M. Shashidhar, V. S. Raja, and B. V. Kumar appeared in the proceedings of the 2011 International Conference on Computer Science and Network Technology (CSNT), June 473–478.

[13] "Brain tumor detection using unsuppler- vised learning based neural network," in Proceedings of the 2013 International Conference on Computer Science and Network Technology (CSNT), pages 573–577, by S. Goswami and L. K. P. Bhaiya.

[14] "A survey of feature selection and feature extraction techniques in machine learning," in Proc. Sci. Inf. Conf., Aug. 2014, pp. 372-378, by S. Khalid, T. Khalil, and S. Nasreen.

Deep learning: Methods and applications, by L. Deng and D. Yu, published in Found. Trends Signal Process, volume 7, issues 3–4, pages 197–387, June 2014.

Referenced in [16] by Y. Lacuna (2015). Convolutional Neural Networks (CNNs), Lenet-5.Lastupdated: 2019.[On the web]. This information is accessible at: HTTP://yann.lecun.com/exdb/lenet. A

[17] The paper "Subject independent facial expression recognition with robust face detection using a convoy-luminal neural network" was written by M. Mitsugi, K. Mori, Y. Mitarai, and Y. Kaneda. (Neuronal Networks), July 2003, vol. 16, no. 5-6, pp. 555-559.

[18] "Deep learning," by Y. Lacuna, Y. Bagnio, and G. Hinton, published in Nature in 2015, volume 521, issue 7553, page 436.

The year 19 The article "Gradient-based learn-Ing applied to document recognition" was published in November 1998 in the Proceedings of the IEEE and was written by Y. Lacuna, L. Bottom, Y. Bagnio, and P. Haffner.20 "ImageNet classification with deep convolutional neural networks," by A. Hrushevsky, I. Subsieve, and G. E. Hinton, published in 2012 in Proc. Adv. Neural Inf. Processing Syst. (NIPS), pages 1097–1105.

in "Classi ⇖cation of brain tumour type and grade using MRI texture and shape in a machine learning scheme," E. I. Zacharaki, S. Wang, S. Chawla, D. S. You, R. Wolf, E. R. Melhem, and C. Davanzo published in Magn. Reason. Med., volume 62, issue 6, pages 1609-1618, December 2009.

A. B. M. Salem, T. Hosny, and E. S. A. El-Dashan, "Hybrid intelligent techniques for MRI brain images classification," [22] Digital Signal Processing, March 2010, volume 20, pages 433–441.

Citation: "Enhanced performance of brain tumour classification via tumour region augmentation and partition" (J. Cheng et al., 2003). Published in October 2015, article number e0140381, in the journal Plops ONE.

Proc. AMIA Annu.Symp. Proc., vol. 2015, Nov. 2015, pp. 1899-1908, "Automated grading of gliomas using deep learning in digital pathology images: A modular approach with ensemble of convolutional neural networks" (24), M. G. Ertegun and D. L. Rubin.

Deep learning for brain tumor classification, by J. S. Paul, A. J. Placard, B. A. Landman, and D. Fabbri [25] Volume 10, issue 3, March 2017, article number 1013710 of Proc. SPIE, Medical Imaging, Biomed. Appl. Mol., Struct.,Functor. Image. Citation: 10.1117/12.2254195.